Tropospheric Refraction Calibrations and Their Significance on Radio-Metric Doppler Reductions

F. B. Winn
Tracking and Orbit Determination Section

The tropospheric refraction algorithm used in the Mariner Mars 1971 tracking data reductions—the orbit determination effort: (1) it differs from previous models used in support of past missions, and (2) it performs two times better than the stated mission requirement.

Although single-pass reductions of doppler tracking data are extremely influenced by tropospheric refraction models, fits to doppler acquired over large time periods, weeks or months, are influenced only slightly: in that, the tropospheric refraction corruption of the doppler observables simply is left in the after-the-fit observed minus computed residuals.

I. Introduction

This report provides a comparison of the tropospheric refraction functions used in the MV67[1], MM69[2], and MM71[3] tracking data reductions in support of the associated orbit determination efforts. The comparisons of the calibration functions are accomplished by noting their relative influences on the least-squares adjustments of solved-for parameters and their ability to represent doppler observations.[4]

[1]MV67: Mariner 5, 1967 (Venus probe).

[2]MM69: Mariners 6 and 7, 1969 (Mars probe).

[3]MM71: Mariner 9, 1971 (Mars probe).

[4]All doppler data employed in this work are fully calibrated for charged particle effects which occur in the Earth's ionosphere or in the plasma clouds of interplanetary space (Refs. 1 and 2).

II. Tropospheric Calibration Functions

In support of the deep space missions, MV67, MM69, and MM71, the following tropospheric refraction calibration functions were used:

$$\text{For MV67: } \Delta\rho_r = N_i(1.8958/340)\,(\sin(\gamma) + 0.6483)^{-1.4} \tag{1}$$

$$\text{For MM69: } \Delta\rho_r = N_i(2.6/340)\,(\sin(\gamma) + 0.015)^{-1} \tag{2}$$

$$\text{For MM71: } \Delta\rho_r = Z_i(t)\,[\sin(\gamma) + 0.00143\,(\tan(\gamma) + 0.0445)^{-1}]^{-1} \tag{3}$$

where

$Z_i(t)$ = a polynomial in time expressing the zenith range error due to retardation.

γ = elevation angle

N_i is a scalar unique to each deep space station:

DSS	N_i
11, 12, 14	240
42	310
61	300

Doppler calibrations for tropospheric refraction are computed from the one-way range corrections, Eqs. (1), (2), (3), in the following manner:

$$\Delta\dot{\rho}_r = \frac{(\Delta\rho_{r_1} + \Delta\rho_{r_3}) - (\Delta\rho_{r_2} + \Delta\rho_{r_4})}{2\,T_c} \qquad (4)$$

where $\Delta\rho_i$, $i = 1, 2, 3, 4$ are the one-way range corrections to be applied to each up or down leg (ρ_i, $i = 1,2,3,4$) of the DSS–spacecraft round-trip transmission (Fig. 1).

III. Analysis

The function (3) is a quite accurate approximation[5] to the system of tables used in the DPODP (Ref. 5) to scale the variable zenith-range-errors to reflect the increased troposphere encountered at lower elevations: all three of these functions will be employed in this study in the *Surveyor* data analysis and the DPODP tables will be used for the MM71 data analysis of this study.

A visual comparison of the three doppler calibration functions is obtainable from Fig. 2. Figure 2 provides the doppler calibrations computed from Eqs. (1), (2), and (3) for DSS 11 tracking a spacecraft at 0-deg declination and at an infinite distance. At 10-deg elevation the functions differ by ~9% to 24%. It is easy to dramatize the significance of these differences. The Hamilton-Melbourne filter (Ref. 6) is capable of expressing these single-pass, doppler calibrations, as equivalent DSS location displacements, $\Delta\lambda$ (longitude) and Δr_s (distance of DSS from the Earth's rotational axis) and additional $\Delta\dot{\rho}$ (the geocentric velocity of the probe).

[5]C. C. Chao states that the functions are within 1% of the Satellite Tracking Orbit Determination Program (SATODP) tables for observations above 1 deg elevation.

Table 1 provides a comparison of the Hamilton–Melbourne representations of the three models for Fig. 2. Table 1 reveals r_s to be the most influenced and $\Delta\lambda$ experienced a displacement at the meter level.

The correlation between r_s and each of the three refraction calibration function scalers (N_i and/or Z_i) is ~0.9 for individual or single pass solutions (Ref. 7). The correlation between r_s and $N_i(Z_i)$ diminishes to ~0.6 for full lunation fits in which 13 to 16 passes of doppler tracking data are reduced simultaneously. The correlation between r_s and N_i (or Z_i) is large enough in the single-pass fits to preclude solving for both r_s and tropospheric refraction scaler in one reduction. This is not the circumstance, however, when an entire lunation of doppler is reduced. The correlation between λ and N_i (or Z_i) is approximately 0.3 for the single-pass doppler solutions and changes little as the number of passes of doppler data increases.

When *Surveyor* doppler tracking data is fit,[6] pass by pass, all structure appears absent from the observed-minus computed doppler residuals (O − C)s after reduction regardless of choice of tropospheric refraction model used. The mean standard deviation, $\sqrt{\Sigma(O-C)^2/n}$, is $\sim 5.4 \times 10^{-2}$ mm/sec for the average single pass, doppler reduction [$\Sigma(O-C)/n \approx 0$]. This is about two times the theoretical limit of the high frequency noise for 300-sec count time, doppler using a rubidium oscillator as the frequency standard (Ref. 8).

The ability of the DSS location parameters, r_s and λ, to absorb the doppler corruptions generated by tropospheric refraction modeling errors yields DSS location solutions which differ from pass solution to pass solution: this is principally due to the data acquisition patterns which vary from pass to pass, and in addition, the tropospheric refraction modeling error[7] is also varying from pass to pass (Table 2). As examples, pass 14 for *Surveyor 6* has no data acquired below 30 deg elevation and pass 4 for *Surveyor 6* has data acquired at an elevation angle of 6 deg.

When 13 to 16 doppler passes are reduced simultaneously the parameter set (in this case DSS locations)

[6]Solutions for r_s and λ only.

[7]Model errors stem from two sources: (1) the model represents an average ideal troposphere while the actual troposphere behavior varies about the mean with time, and (2) the model's behavior relative to the "real mean" troposphere is dependent upon the elevation span associated with the doppler observables over a pass.

fails to fit the doppler observables (Ref. 9). That is, although the solution parameter adjustments are influenced by the choice of tropospheric refraction calibration function, much of the "diurnal" or "elevation" signature remains in the doppler (O − C) residuals. The standard deviation associated with the full lunation doppler reduction is $\sim 4 \times 10^{-1}$ mm/sec or eight times greater than for the single-pass fits.

Likewise, the long trajectory data fits to the parameter sets associated with MM71 demonstrate characteristics similar to those shown by the *Surveyor* lunation data fits: the (O − C)s after the fit exhibit "tropospheric refraction" type structures (Fig. 3). Comparison of "B-plane" position estimates (Ref. 10) of *Mariner 9* as a function of tropospheric refraction model is the subject of Table 3. DSS location solutions experienced displacements near the meter level.

It appears that the preponderence of the tropospheric modeling error is clearly left in the (O − C)s after the fit.

It should be stated that the tropospheric refraction modeling errors mentioned above result in an integrated range error of ~0.5 m 70% of the time (for doppler above 5 deg elevation). This corresponds to a one sigma of ~0.5 m/pass which is a factor of 2 better than the MM71 mission requirement (Ref. 11).

IV. Conclusions

The tropospheric refraction algorithm performs within mission requirements; however, tropospheric refraction type structures still reside in the (O − C)s after the fit having amplitudes frequently of 0.3 to 0.4 mm/sec.

Although single-pass reductions of doppler tracking data are extremely influenced by tropospheric refraction models, fits to doppler acquired over large time periods, weeks or months, are influenced only slightly, in that the tropospheric refraction corruption of the doppler observables simply is left in the after-the-fit observed minus computed residuals.

References

1. Mulhall, B. D., et al., "The Ionosphere," in *Tracking System Analytic Calibration Activities for the Mariner Mars 1969 Mission,* Technical Report 32-1499, Jet Propulsion Laboratory, Pasadena, Calif., Nov. 15, 1970.
2. MacDoran, P. F., "A First-Principles Derivation of the Differenced Range Versus Integrated Doppler (DRVID) Charged Particle Calibration Method," in *The Deep Space Network,* Space Programs Summary 37-62, Vol. II, pp. 28–33. Jet Propulsion Laboratory, Pasadena, Calif., March 31, 1970.
3. Miller, L. F., Ondrasik, V. J., Chao, C. C., "A Cursory Examination of the Sensitivity of the Tropospheric Range and Doppler Effects to the Shape of the Refractivity Profile," in *The Deep Space Network,* Technical Report 32-1526, Vol. I, pp. 22–30. Jet Propulsion Laboratory, Pasadena, Calif., Feb. 15, 1971.
4. Chao, C. C., "New Tropospheric Range Corrections With Seasonal Adjustment," in *The Deep Space Network,* Technical Report 32-1526, Vol. VI, pp. 67–73. Jet Propulsion Laboratory, Pasadena, Calif., Dec. 15, 1971.
5. Moyer, T. D., *Mathematical Formulation of the Double-Precision Orbit Determination Program (DPODP),* Technical Report 32-1527. Jet Propulsion Laboratory, Pasadena, Calif., May 15, 1971.
6. Hamilton, T. W., and Melbourne, W. G., "Information Content of a Single Pass of Doppler Data From a Distant Spacecraft," in *The Deep Space Network,* Space Programs Summary 37-39, Vol. III, pp. 18–33. Jet Propulsion Laboratory, Pasadena, Calif., May 31, 1966.

References (contd)

7. Winn, F. B., and Leavitt, R. K., "Refractivity Influence on DSS Doppler Data," in *The Deep Space Network*, Technical Report 32-1526, Vol. I, pp. 31–41. Jet Propulsion Laboratory, Pasadena, Calif., Feb. 15, 1971.

8. Trask, D. W., and Hamilton, T. W., "Tracking Data Inherent Accuracy Analysis: DSIF Two-Way Doppler Inherent Accuracy Limitations," in *The Deep Space Network*, Space Programs Summary 37-38, Vol. III, pp. 8–13. Jet Propulsion Laboratory, Pasadena, Calif., March 31, 1966.

9. Winn, F. B., "Surveyor Post-Touchdown Analysis of Tracking Data," in *Surveyor Project Final Report, Part II: Science Results*, Technical Report 32-1265, Jet Propulsion Laboratory, Pasadena, Calif., June 15, 1968.

Table 1. Comparison of doppler calibration functions for refraction

Functions	$\delta(\Delta r_s)$	$\delta(\Delta\lambda)$	$\delta(\Delta\dot{r})$
1 − 2	5.12 m	0.80 m	0.10 mm/s
1 − 3	3.44 m	0.51 m	0.04 mm/s
2 − 3	8.56 m	1.31 m	0.14 mm/s

$\dot{r}$ = geocentric radial velocity of probe.

δ = difference of coordinate adjustments resulting from refraction modeling.

Table 2. Single-pass doppler fits with different refraction models

	Function 1 − 2		Function 2 − 3		Function 1 − 3	
Pass	$\delta(\Delta r_s)$	$\delta(\Delta\lambda)$	$\delta(\Delta r_s)$	$\delta(\Delta\lambda)$	$\delta(\Delta r_s)$	$\delta(\Delta\lambda)$
3	3.04 m	−0.32 m	−1.53 m	+0.27 m	−4.57 m	+0.59 m
4	6.04	−3.69	−3.72	+2.79	−9.76	+6.48
5	2.90	−0.51	−1.42	−1.14	−4.32	−0.63
6	4.77	−0.93	−3.37	+0.62	−8.14	+1.55
7	3.79	+0.73	−1.27	−0.53	−5.06	−1.26
8	2.92	−1.25	−1.36	+0.87	−4.28	+2.12
9	2.05	−0.40	−0.71	+0.29	−2.76	+0.69
10	2.12	+0.11	−0.79	−0.13	−2.91	−0.24
11	1.78	−0.16	+0.61	+0.09	−2.39	+0.25
12	1.96	−0.25	−0.76	+0.15	−2.72	+0.40
13	0.90	−0.02	+0.07	+0.00	−0.83	+0.02
14	1.11	+0.05	+0.01	−0.02	−1.12	−0.07
15	1.02	+0.03	+0.02	+0.01	−1.00	−0.02

δ = the difference of the adjustments called for by different refraction models

Table 3. Comparison of tropospheric modeling changes on a *Mariner 9* long arc doppler solution

Station parameter	Δ
r_s	0.8 m
λ	0.2 m
$B \cdot R$	4.5 km
$B \cdot T$	0.6 km

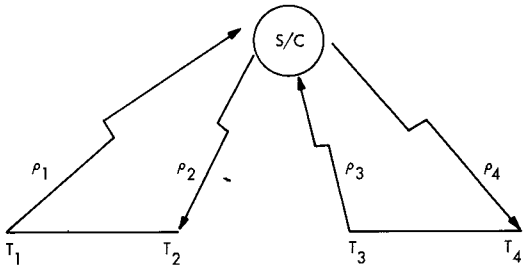

DSS DOPPLER COUNT TIME $T_C = T_4 - T_2$
$= T_3 - T_1$

Fig. 1. Doppler computations

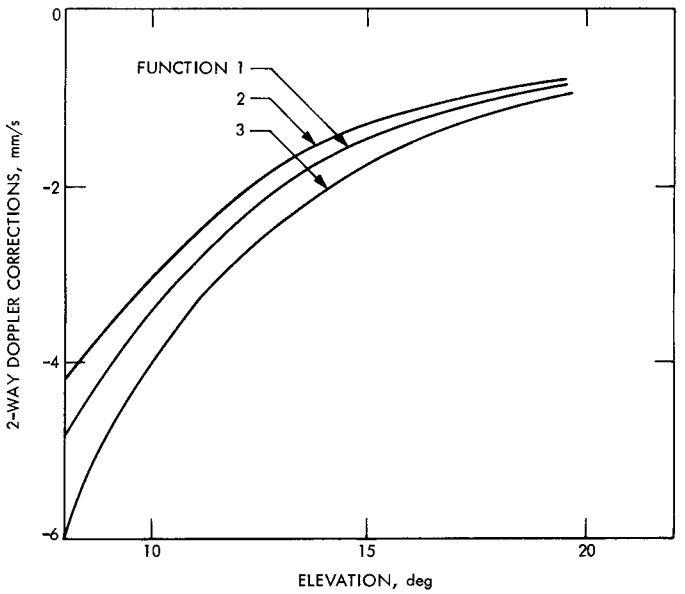

Fig. 2. Refraction functions

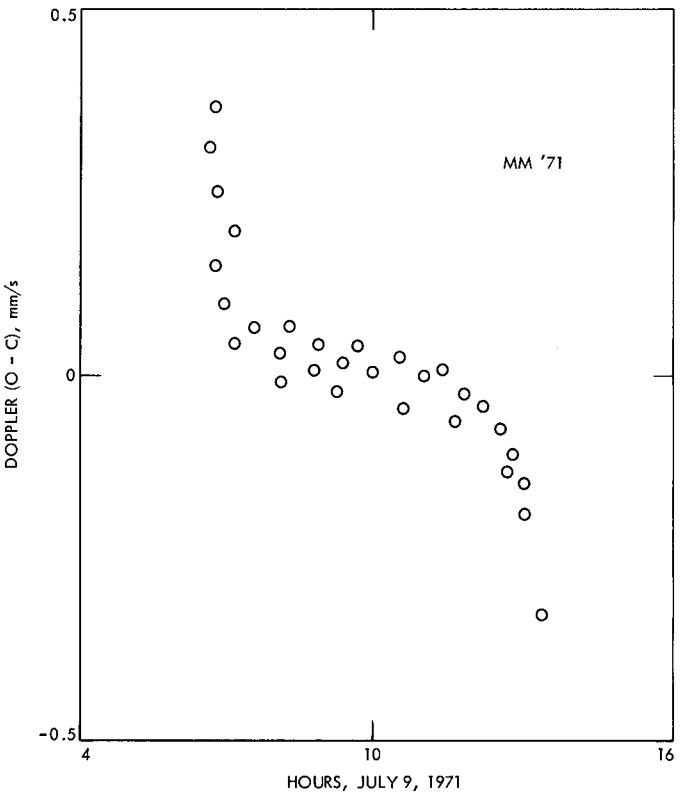

Fig. 3. Typical after-the-fit doppler (O — C) signatures